Heliyon 5 (2019) e01827

Contents lists available at ScienceDirect

Heliyon

www.elsevier.com/locate/heliyon

H_∞/LPV controller design for an active anti-roll bar system of heavy vehicles using parameter dependent weighting functions

Van Tan Vu [a,*], Olivier Sename [b], Luc Dugard [b], Peter Gaspar [c]

[a] Department of Automotive Mechanical Engineering, University of Transport and Communications, Hanoi, Viet Nam
[b] Univ. Grenoble Alpes, CNRS, Grenoble INP (Institute of Engineering Univ. Grenoble Alpes), GIPSA-lab, 38000 Grenoble, France
[c] Systems and Control Laboratory, Institute for Computer Science and Control, Hungarian Academy of Sciences, Budapest, Hungary

ARTICLE INFO

Keywords:
Vehicle dynamics
Active anti-roll bar system
Linear Parameter Varying
H_∞/LPV control
Roll stability
Vehicle rollover

ABSTRACT

Vehicle rollover is a very serious problem when considering the safety of heavy vehicles, which can result in large financial and environmental consequences. This paper investigates the interest of a Linear Parameter Varying (LPV) controller for an active anti-roll bar system of single unit heavy vehicles, in order to enhance roll stability. We propose a parameter dependent H_∞/LPV controller with weighting functions, scheduled by the forward velocity (the varying parameter of the vehicle LPV model) and by the normalized load transfers at the two axles (part of the parameter dependent weighting functions) providing an on-line performance adaptation to the vehicle rollover risk. The effectiveness of the proposed controller is validated by using the TruckSim® simulation software with two different types of heavy vehicle: a fully loaded bus and a truck. The simulation results, in the frequency and time domains, show that the proposed strategy drastically improves the vehicle roll stability when compared with a H_∞/LTI controller, a fixed weighting functions H_∞/LPV controller and a passive anti-roll bar system.

1. Introduction

Rollover of heavy vehicles is still an important road safety problem world-wide. Although rollovers are relatively rare events, they may be fatal accidents. According to the Federal National Highway Traffic Safety Administration (NHTSA), in the United States, there were 333,000 heavy vehicles involved in traffic crashes during 2012. Rollover crashes were responsible of 3,921 fatal accidents and 104,000 injuries (an increase of 18 percent from 2011). From 2012 to 2016, rollover occurrence (for single unit and combination unit vehicles) is about 15% in fatal crashes.

While rollover accidents may occur, due mainly to side wind gusts, abrupt steering and/or braking manoeuvres, they result, for heavy vehicles, from the loss of roll stability (when the tyre-road contact force at one of the side wheels becomes zero).

Rollover accidents can be grouped into four classifications: preventable, potentially preventable, non-preventable and prevention unknown [1]. It is typically hard for the driver of a heavy vehicle to detect the start of a rollover event. Many rollover situations cannot be prevented by driver's actions alone, even when they are correctly warned through the warning devices. To prevent rollover, several active control schemes have been proposed: active steering [2], active braking [3], active suspension [4, 5] and active anti-roll bars [6], the latter being the most common method used for heavy vehicles.

Active anti-roll bar systems use active components to control the vehicle roll behaviour, and they are often made up of a pair of hydraulic actuators, in order to determine the variation in the equivalent stiffness of the anti-roll bars. The vehicle load distribution is influenced by the roll-bar stiffness distribution. Unlike the passive anti-roll bar system, the active anti-roll bar system generates a stabilizing moment to counterbalance the overturning moment in such a way that the control torque leans the vehicle into the corners [7, 8]. The advantage of this system is that it requires much lower bandwidth of the hydraulic actuators and a simpler control strategy than other systems that attempt to control all vehicle modes. However, because the relative roll angle of the suspension is limited to about 8 degrees, the maximum stabilizing moment that is created cannot be too large [9].

The LPV approach is considered in this paper. It is known to be able to handle system non linearities by considering them as varying parameters and, as well, to make the controller performances varying through the linear introduction of smart (high-level) parameters, as illustrated in [10] for instance, or in several chapters in the books [11, 12].

* Corresponding author.
E-mail address: vvtan@utc.edu.vn (V.T. Vu).

https://doi.org/10.1016/j.heliyon.2019.e01827
Received 29 August 2018; Received in revised form 12 April 2019; Accepted 23 May 2019

Here, the present work proposes a MIMO LPV control synthesis method which makes use of a LPV integrated model of a single unit vehicle ([13]) and which accounts for the rollover risk through the choice of parameter dependent H_∞ weighting functions which depend on the front and rear normalized load transfers.

1.1. Related works

Many control strategies have been developed for the active anti-roll bar system of single unit heavy vehicles, using the yaw-roll model, as shown below.

Optimal control: In [9, 14, 15] the authors used the *LQR* method. The control torques acting between the axle groups and the sprung mass are considered as the input control signals. The simulation results indicate that the normalized load transfers at all the axles reduce significantly, compared with the passive anti-roll bar system at 60 km/h. In [13, 16] the authors have proposed an integrated model with four electronic servo-valve hydraulic actuator models in a single unit heavy vehicle yaw-roll model. Then the LQR control method was applied to the active anti-roll bar, so demonstrating how it may solve a multi-objective problem by considering the improvement of the roll stability, while taking into account the characteristics of the electronic servo-valve hydraulic actuators.

H_∞ and LPV control: In [7, 17] the LPV approach was applied for the active anti-roll bar system combined with the active braking system. The forward velocity was considered as the varying parameter. The different actuator failures are identified by using a Fault Detection and Identification *(FDI)* filter.

1.2. Paper contributions and organisation

The main contributions of this paper are summarized below:

- For the first time, a MIMO parameter dependent weighting functions H_∞/LPV controller, with three varying parameters (forward velocity together with the front and rear normalized load transfers) is considered to allow for performance adaptation to the rollover risk of heavy vehicles, characterized by the normalized load transfers at the two axles. Frequency and time domain analyses indeed show that the parameter dependent weighting functions H_∞/LPV controller is a realistic solution which drastically improves the vehicle roll stability when compared with the H_∞/LTI, fixed weighting functions H_∞/LPV controllers and the passive anti-roll bar system.
- The proposed H_∞/LPV controller is validated using the TruckSim® simulation software with two different types of vehicle: a fully loaded tour bus and a fully loaded LCF (Low Cab Forward) truck. Since the rollover risk changes from trucks to buses, the LPV controller can adapt the performance against this rollover risk for all types of heavy vehicles.

This paper is organised as follows: Section 2 details the LPV model of a single unit heavy vehicle with the forward velocity as a scheduling parameter. Section 3 is devoted to methodology with the formulation of the H_∞/LPV control problem. In section 4, one gives the theoretical background which allows then to compute the H_∞/LPV control law. Section 5 is concerned by the analysis of the closed-loop system in the frequency and time domains. The results and associated discussion, of a realistic validation of the H_∞/LPV controller using the TruckSim® simulation software are presented in section 6. Finally, some conclusions are drawn in section 7.

2. Model

Vehicle modelling is performed using the LPV approach. We briefly recall here the integrated model of a single unit heavy vehicle, previously detailed in [13]. It includes the Yaw-Roll model proposed in [17] (see also references in [13]). This model is then rewritten in a LPV form.

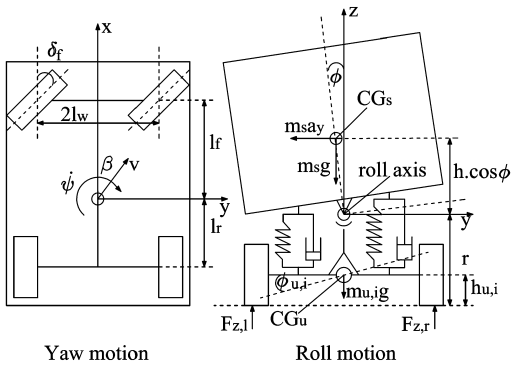

Fig. 1. Yaw-roll model of a single unit heavy vehicle.

2.1. The integrated model

The considered model merges the yaw-roll model (firstly developed in [17]) with Electronic Servo-Valve Hydraulic (ESVH) actuators (at the front and at the rear axles). The symbols and the parameter values of the integrated model are given in [13].

First, from [13], the dynamical equations of the ESVH actuators given as follows:

$$\begin{cases} \frac{V_t}{4\beta_e}\dot{\Delta}_{Pf} + (K_P + C_{tp})\Delta_{Pf} - K_x X_{vf} + A_p l_{act}\dot{\phi} - A_p l_{act}\dot{\phi}_{uf} = 0 \\ \dot{X}_{vf} + \frac{1}{\tau}X_{vf} - \frac{K_v}{\tau}u_f = 0 \\ \frac{V_t}{4\beta_e}\dot{\Delta}_{Pr} + (K_P + C_{tp})\Delta_{Pr} - K_x X_{vf} + A_p l_{act}\dot{\phi} - A_p l_{act}\dot{\phi}_{ur} = 0 \\ \dot{X}_{vr} + \frac{1}{\tau}X_{vr} - \frac{K_v}{\tau}u_r = 0 \end{cases} \quad (1)$$

where u_f and u_r are the control signals of the ESVH actuator (i.e. the electrical current opening the electronic servo-valve).

The linear yaw-roll model is shown in Fig. 1 [17]. The differential equations of motion, i.e., the lateral dynamics, the yaw moment, the roll moment of the sprung mass, the roll moment of the unsprung masses at the two axles, are formalized in the equations (2):

$$\begin{cases} mv(\dot{\beta}+\dot{\psi}) - m_s h\ddot{\phi} = F_{yf} + F_{yr} \\ -I_{xz}\ddot{\phi} + I_{zz}\ddot{\psi} = F_{yf}l_f - F_{yr}l_r \\ (I_{xx} + m_s h^2)\ddot{\phi} - I_{xz}\ddot{\psi} = m_s v h(\dot{\beta}+\dot{\psi}) \\ \quad +m_s g h\phi - k_f(\phi - \phi_{uf}) - b_f(\dot{\phi} - \dot{\phi}_{uf}) \\ \quad +T_f - k_r(\phi - \phi_{ur}) - b_r(\dot{\phi} - \dot{\phi}_{ur}) + T_r \\ -rF_{yf} = m_{uf} v(r - h_{uf})(\dot{\beta}+\dot{\psi}) \\ \quad +m_{uf} g h_{uf}.\phi_{uf} - k_{tf}\phi_{uf} \\ \quad +k_f(\phi - \phi_{uf}) + b_f(\dot{\phi} - \dot{\phi}_{uf}) + T_f \\ -rF_{yr} = m_{ur} v(r - h_{ur})(\dot{\beta}+\dot{\psi}) - m_{ur} g h_{ur}\phi_{ur} \\ \quad -k_{tr}\phi_{ur} + k_r(\phi - \phi_{ur}) + b_r(\dot{\phi} - \dot{\phi}_{ur}) + T_r \end{cases} \quad (2)$$

where T_f and T_r are the torques generated by the active anti-roll bar system at the front and rear axles. The lateral tyre forces $F_{yf,r}$ in the direction of velocity at the wheel ground contact points are modelled by a linear stiffness as:

$$\begin{cases} F_{yf} = \mu C_f(-\beta + \delta_f - \frac{l_f\dot{\psi}}{v}) \\ F_{yr} = \mu C_r(-\beta + \frac{l_r\dot{\psi}}{v}) \end{cases} \quad (3)$$

The torque generated by the active anti-roll bar system [13] at the front and rear axles are determined by: $T_f = 2l_{act}F_{actf} = 2l_{act}A_p\Delta_{Pf}$, $T_r = 2l_{act}F_{actr} = 2l_{act}A_p\Delta_{Pr}$, where Δ_{Pf} and Δ_{Pr} are respectively the difference of pressure of the hydraulic cylinder at the front and rear axles.

2.2. An LPV model of a single unit heavy vehicle

We can see in (2)–(3) that the yaw-roll model depends on the forward velocity v and on the inverse of the forward velocity $\frac{1}{v}$. Moreover, when the vehicle is in motion, the forward velocity is one of the constantly changing parameters, and it depends on the driver and the motion condition of the vehicle. Here, the forward velocity v is chosen as a scheduling parameter.

Denoting $\rho_1 = v$ the integrated model (1)–(3) can be rewritten as the Linear Parameter Varying system:

$$\dot{x} = A(\rho_1).x + B_1(\rho_1).w + B_2(\rho_1).u \tag{4}$$

with x the state vector:

$$x = \begin{bmatrix} \beta & \dot{\psi} & \phi & \dot{\phi} & \phi_{uf} & \phi_{ur} & \Delta_{Pf} & X_{vf} & \Delta_{Pr} & X_{vr} \end{bmatrix}^T.$$

The exogenous disturbance (steering angle) is: $w = \begin{bmatrix} \delta_f \end{bmatrix}^T$ and the control inputs (input currents) are: $u = \begin{bmatrix} u_f & u_r \end{bmatrix}^T$.

Remark. The matrix $A(\rho_1)$ is not affine in ρ_1 since it includes ρ_1 and $\frac{1}{\rho_1}$. Therefore the classical polytopic approach cannot be used unless we consider two different parameters, which increases the conservatism.

3. Methodology

The control problem is formulated in the H_∞/LPV framework. We detail the performance specification and criteria that lead to the H_∞/LPV control problem.

3.1. Performance criteria and scheduling strategy

The rollover occurs when $F_z = 0$ (the tyre force in the Z direction at each wheel), i.e. when the wheel starts to lift off the road. However the value of F_z is not easy to measure or to estimate.

Usually, for heavy vehicles, the rollover is evaluated from the normalized load transfers $R_{f,r}$ (5) at the two axles, as presented in [7, 18, 19]. For the yaw-roll model in Fig. 1 we then define:

$$R_f = \frac{\Delta F_{zf}}{F_{zaf}}, \quad R_r = \frac{\Delta F_{zr}}{F_{zar}} \tag{5}$$

where F_{zaf} is the total axle load at the front axle and F_{zar} at the rear axle. ΔF_{zf} and ΔF_{zr} are respectively the lateral load transfers at the front and rear axles, which can be given in the equation (6).

$$\Delta F_{zf} = \frac{k_{uf}\phi_{uf}}{l_w}, \quad \Delta F_{zr} = \frac{k_{ur}\phi_{ur}}{l_w} \tag{6}$$

Therefore, when the value of $R_{f,r}$ takes on the limit of ± 1, the wheel in the inner bend lifts off the road and the rollover occurs.

It is worth noting that, in case of obstacle avoidance, the wheels at the rear axle lift off first for the truck, due to higher suspension ratio stiffness to load, which is greater at the rear axle than at the front one [6], [7]. However the other effect to be considered in vehicle rollover, is the distribution of the total load for the two axles. In the case of big buses, the engine is often mounted at the rear, so the wheels at the front axle usually lift off first. Therefore it is generally necessary to consider the rollover risk at the two axles of heavy vehicles.

Since such performance indices are the key parameters to evaluate the risk of rollover, both are considered, for the first time, as scheduling parameters of the LPV control, in order to provide a stable and smooth control action when reaching critical situations. Let us note that a similar idea was used in [7], [17] considering the rear load transfer only in order to account for actuator fault and to switch on braking actuations when critical situations occur.

We then define $\rho_2 = |R_f|$ and $\rho_3 = |R_r|$.

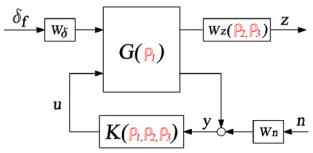

Fig. 2. The closed-loop interconnection structure of the LPV active anti-roll bar control.

3.2. Performance specifications for the H_∞/LPV control design

In Fig. 2, the given H_∞/LPV control structure includes the nominal model $G(\rho_1)$, the controller $K(\rho_1, \rho_2, \rho_3)$, the performance output z, the control input u, the measured output y and the measurement noise n. The steering angle δ_f is the disturbance signal, set by the driver. The weighting functions $W_\delta, W_z(\rho_{2,3}), W_n$ are presented thereafter, according to the considered performance objectives.

The weighting functions matrix W_z representing the performance output, is chosen as $W_z = diag[W_{zu}, W_{zR}]$. The purpose of the weighting functions is to keep the control inputs and normalized load transfers as small as possible over the desired frequency range up to 4 rad/s, which represents the limited bandwidth of the driver [7, 9]. These weighting functions can be considered as penalty functions, that is, weights which should be large in the frequency range where small signals are desired and small where larger performance outputs can be tolerated.

The weighting function W_{zu}, dedicated to the input currents at the front and rear axles, allows to account for actuator limitations. W_{zu} is selected as the equation (7):

$$W_{zu} = diag[W_{zuf}, W_{zur}]; \quad W_{zuf} = \frac{1}{\eta_{uf}}; \quad W_{zur} = \frac{1}{\eta_{ur}} \tag{7}$$

with $\eta_{uf} = \eta_{ur} = 0.4$.

The weighting function W_{zR}, chosen as $W_{zR} = diag[W_{zRf}, W_{zRr}]$, corresponds to the normalized load transfers at the front and rear axles and is selected as:

$$W_{zRf} = \rho_2 \frac{s\vartheta_{Rf} + 1}{s\lambda_{Rf} + \chi_{Rf}}; \quad W_{zRr} = \rho_3 \frac{s\vartheta_{Rr} + 1}{s\lambda_{Rr} + \chi_{Rr}} \tag{8}$$

Here, the equations (8) are chosen as simple first-order systems (to limit the controller complexity) in order to limit the load transfers in the frequency range of interest, with: $\vartheta_{Rf} = \vartheta_{Rr} = 0.05$; $\lambda_{Rf} = \lambda_{Rr} = 0.01$; $\chi_{Rf} = \chi_{Rr} = 15$.

We stress that the interest of parameter dependant weighting functions is to allow for performance adaptation to the rollover risk of heavy vehicles. Indeed, the ESVH actuators will be tuned according to the varying parameters in order to meet the desired performance. For example, as far as the normalized load transfer at the front is concerned, when the varying parameter $\rho_2 \to 1$, the gain of the weighting function W_{zRf} is large, and therefore the normalized load transfer at the front is penalized. In the same way, when ρ_3 is large, the normalized load transfer at the rear will be reduced.

The input scaling weight W_δ normalizes the steering angle to the maximum expected command. It is selected as $W_\delta = \pi/180$, which corresponds to a 1^0 steering angle command.

The weighting function W_n is selected as a diagonal matrix which accounts for sensor noises. The noise weights are chosen as 0.01 (m/s^2) for the lateral acceleration and $0.01(^0/sec)$ for the derivative of the roll angle $\dot{\phi}$ [7].

3.3. The LPV generalized plant

According to Fig. 2, the concatenation of the nonlinear model (4) with the performance weighting functions leads to the generalized plant:

$$\begin{bmatrix} \dot{x}(t) \\ z(t) \\ y(t) \end{bmatrix} = \begin{bmatrix} A(\rho) & B_1(\rho) & B_2(\rho) \\ C_1(\rho) & D_{11}(\rho) & D_{12}(\rho) \\ C_2(\rho) & D_{21}(\rho) & D_{22}(\rho) \end{bmatrix} \begin{bmatrix} x(t) \\ w(t) \\ u(t) \end{bmatrix} \tag{9}$$

with the exogenous input $w(t) = \begin{bmatrix} \delta_f & n \end{bmatrix}$, the control input $u(t) = \begin{bmatrix} u_f & u_r \end{bmatrix}^T$, the measured output vector $y(t) = \begin{bmatrix} a_y & \dot{\phi} \end{bmatrix}^T$ and the performance output vector $z(t) = \begin{bmatrix} u_f & u_r & R_f & R_r \end{bmatrix}^T$.

It is worth noting that, in the LPV model of the active anti-roll bar system (9), the varying parameters $\rho = [\rho_1, \rho_2, \rho_3]$ are known in real time. Indeed the parameter $\rho_1 = v$ is measured directly, while the parameters $R_{f,r}$ (ρ_2 and ρ_3) can be calculated by using the measured roll angle of the unsprung masses $\phi_{uf,r}$ [7].

3.4. H_∞/LPV control problem

The control goal is to find an LPV controller $K(\rho)$ defined as:

$$\begin{bmatrix} \dot{x}_K(t) \\ u(t) \end{bmatrix} = \begin{bmatrix} A_K(\rho) & B_K(\rho) \\ C_K(\rho) & D_K(\rho) \end{bmatrix} \begin{bmatrix} x_K(t) \\ y(t) \end{bmatrix} \tag{10}$$

where $A_K(\rho)$, $B_K(\rho)$, $C_K(\rho)$, $D_K(\rho)$ are continuous bounded matrix functions, which minimizes the induced $\mathscr{L}_2$ norm of the closed-loop LPV system $\sum_{CL} = LFT(G, K)$, with zero initial conditions as in the equation (11).

$$\| \sum\nolimits_{CL}(\rho) \|_{2\to 2} = \sup_{\substack{\rho\in\mathscr{P} \\ \bar{\nu}\le\dot{\rho}\le\underline{\nu}}} \sup_{\substack{w\in\mathscr{L}_2 \\ \|w\|_2\neq 0}} \frac{\| z \|_2}{\| w \|_2} \tag{11}$$

The existence of a controller that solves the parameter dependent LPV γ-performance problem can be expressed as the feasibility of a set of linear matrix inequalities (LMIs), which can be solved numerically [7].

It is worth noting that:

- the above problem can be solved by considering the parameter dependent stability of LPV systems, which is the generalization of the quadratic stability concept. Applying the parameter dependent stability concept, it is assumed that the derivative of the parameters can also be measured in real time. This concept is less conservative than the quadratic stability [20, 21, 22].
- the possible controller dependence on $\dot{\rho}$ will be stated by the adopted solution in terms of the parameter-dependence or not, of the Lyapunov matrix.

4. Theory/calculation

4.1. Some background on solving H_∞/LPV control problem

Let us consider the LPV generalized plant (9). First, let recall that several methods have arisen for representing the parameter dependence in LPV models, and then for designing the LPV controllers, such as [23]:

- **Linear Fractional Transformations (LFT)** [24, 25]: LFT models are attractive since they can incorporate a wide set of parameter representations (including rational dependency), together with uncertainties.
- **Polytopic solution**: A polytopic system is a convex combination of systems defined at each vertex of a polytope given by the bounds of the scheduling parameters [26]. The synthesis of such a controller can be made in the H_∞/LPV framework based on the LMI solution for polytopic systems (the framework of quadratic stabilization). This can be applied to LPV systems with an affine dependence on the parameters only.
- **Linearizations on a gridded domain (grid-based LPV)** [20, 26], divide the parameter domain into a grid of its values, and then specify the linear dynamics at each grid point through Jacobian linearization. All the linearized systems on the grid have identical inputs, outputs and state vectors. In the vicinity of each grid point, the linearization is determined to be closest to the system's dynamics, and can therefore capture the system's parameter dependence implicitly. Therefore, the grid-based LPV method can handle any type of parameter representation.

Here, we are interested in the grid-based LPV approach implemented in the LPVTools™ toolbox [27]. Indeed such an approach is interesting when the number of parameters increases since the polytopic approach may lead to very conservative results (due to the augmented size of the parameter set and the single Lyapunov function). It has been used successfully in several studies as for instance in [28].

Some brief recalls on the synthesis of dynamic and feedback controllers for LPV systems are presented below (which corresponds to the implemented method in LPVTools). More details can be found in [20, 21, 22]. The following theorem describes the LPV analysis problem when it is formulated in terms of the induced $\mathscr{L}_2$ norm of $G(\rho)$ and the rate-bounds $(\bar{\nu}, \underline{\nu})$ of the parameter are taken into account [7].

Theorem 1 *([20, 21, 22]). Given a compact set $\mathscr{P} \subset \mathscr{R}^S$, the performance level γ and the LPV system (9), with restriction $D_{11}(\rho) = 0$, the parameter-dependent γ-performance problem is solvable if there exist a continuously differentiable function $X: \mathscr{R}^S \to \mathscr{R}^{n\times n}$, and $Y: \mathscr{R}^S \to \mathscr{R}^{n\times n}$, such that for all $\rho \in \mathscr{P}$, $X(\rho) = X^T(\rho) > 0$, $Y(\rho) = Y^T(\rho) > 0$ and the conditions (12), (13), (14) are satisfied*

$$\begin{bmatrix} \hat{A}(\rho)X(\rho) + X(\rho)\hat{A}^T(\rho) - \sum_{i=1}^{s}(\nu_i \frac{\partial X}{\partial \rho_i}) - B_2(\rho)B_2^T(\rho) & X(\rho)C_1^T(\rho) & \gamma^{-1}B_1(\rho) \\ C_1(\rho)X(\rho) & -I_{ne} & 0 \\ \gamma^{-1}B_1^T(\rho) & 0 & -I_{nd} \end{bmatrix} < 0, \tag{12}$$

$$\begin{bmatrix} \tilde{A}^T(\rho)Y(\rho) + Y(\rho)\tilde{A}(\rho) + \sum_{i=1}^{s}(\nu_i \frac{\partial Y}{\partial \rho_i}) - C_2^T(\rho)C_2(\rho) & Y(\rho)B_1(\rho) & \gamma^{-1}C_1^T(\rho) \\ B_1^T(\rho)Y(\rho) & -I_{nd} & 0 \\ \gamma^{-1}C_1(\rho) & 0 & -I_{ne} \end{bmatrix} < 0, \tag{13}$$

$$\begin{bmatrix} X(\rho) & \gamma^{-1}I_n \\ \gamma^{-1}I_n & Y(\rho) \end{bmatrix} \ge 0 \tag{14}$$

where $\hat{A}(\rho) = A(\rho) - B_2(\rho)C_1(\rho)$, $\tilde{A}(\rho) = A(\rho) - B_1(\rho)C_2(\rho)$. If these conditions are satisfied, there exists a controller (10) which can solve that problem.

The constraints set by the LMIs in Theorem 1 are infinite dimensional, as is the solution space. The variables are X, Y: $\mathscr{R}^S \to \mathscr{R}^{n\times n}$, which restricts the search to the span of a collection of known scalar basis functions. By selecting scalar continuous differentiable basis functions $\{g_i : \mathscr{R}^S \to \mathscr{R}\}_{i=1}^{N_x}$, $\{f_i : \mathscr{R}^S \to \mathscr{R}\}_{j=1}^{N_y}$, then the variables in Theorem 1 can be expressed as:

$$X(\rho) = \sum_{i=1}^{N_x} g_i(\rho)X_i, \quad Y(\rho) = \sum_{i=1}^{N_y} f_i(\rho)Y_j \tag{15}$$

Currently, there is no analytical method to select the basis functions g_i and f_i. An intuitive rule for the basis function selection is to use those present in the open-loop state space data.

4.2. The LPV anti-roll bar control solution

The general LPV system representation (9) depends on an infinite set of parameter values. However, in the grid-based LPV framework, this conceptual representation is considered as a family of the LTI systems obtained for a finite gridded domain (frozen values) of the parameter vector ρ. Each LTI $S(\hat{\rho}_k)$ system is characterized by the matrices ($A(\hat{\rho}_k)$, $B(\hat{\rho}_k)$, $C(\hat{\rho}_k)$ and $D(\hat{\rho}_k)$) at each grid point $\hat{\rho}_k$ ($\hat{\rho}_k$ is fixed) [27]. As mentioned above, the linearized and original LPV systems have the same inputs, outputs and state vectors. Therefore this family of LTI models creates an LPV system approximation of $S(\rho)$ [28, 29].

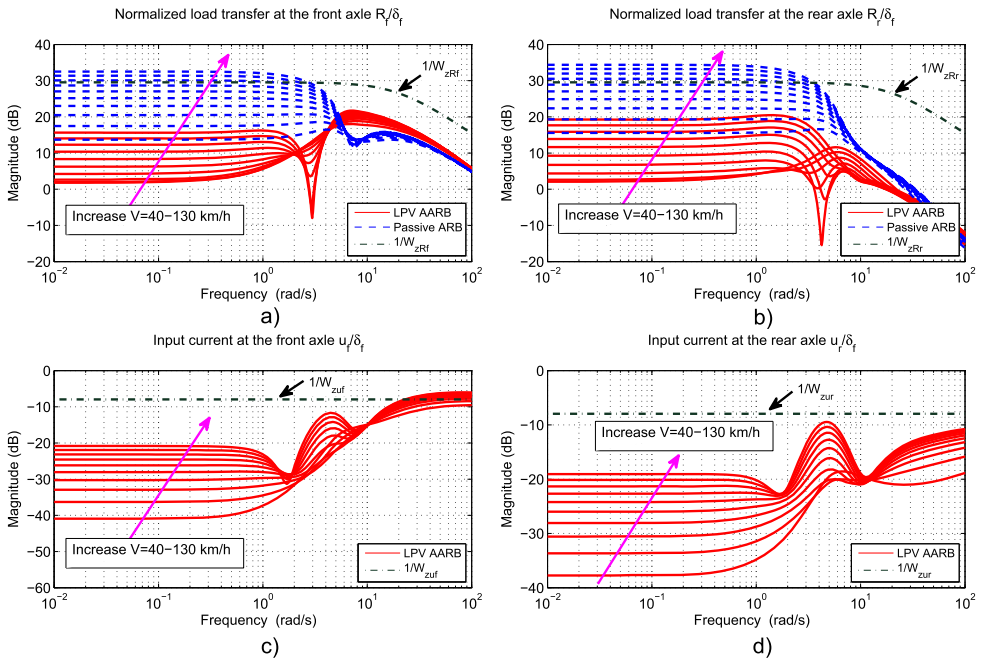

Fig. 3. First case: transfer function magnitude of (a, b) the normalized load transfers $\frac{R_{f,r}}{\delta_f}$, (c, d) the input currents $\frac{u_{f,r}}{\delta_f}$ at the two axles.

The grid-based LPV approach for the active anti-roll bar system

Such a grid-based approach is used here to find an LPV controller (10) solving the Theorem 1. It requires a gridded parameter space for the three varying parameters $\rho = [\rho_1, \rho_2, \rho_3]$. In the interconnection structure, the spacing of the grid points is selected on the basis of how well the H_∞ point designs perform for plants around the design point. The H_∞ controllers are synthesized for 10 grid points of the forward velocity in the range $\rho_1 = v \in [40\ \text{km/h}, 130\ \text{km/h}]$ and 5 grid points of the normalized load transfers at the two axles in a range $\rho_2 = |R_f| \in [0, 1]$, $\rho_3 = |R_r| \in [0, 1]$, respectively.

For simplification, we have first chosen to design a controller that does not depend on the parameter derivatives (so the scalar basis functions (15) are constant). By using the LPVTools™ [27], the following commands are used to make the grid points as well as the LPV controller synthesis:

rho1 = pgrid('rho1',linspace(40/3.6,130/3.6,10));
rho2 = pgrid('rho2',linspace(0,1,5));
rho3 = pgrid('rho3',linspace(0,1,5))
and *[Klpv,normlpv] = lpvsyn(H,nmeas,ncont)*.

The weighting functions for both the performance and robustness specifications are considered unique for the whole grid. The effect of the proposed H_∞/LPV controller to improve the roll stability of heavy vehicles will be proved in the next sections.

5. Analysis

5.1. Frequency domain analysis

Various closed-loop transfer functions of the LPV active anti-roll bar system are shown in this section. Its main objective is to reduce the normalized load transfer at each axle ($R_{f,r}$). To evaluate the effectiveness of the proposed H_∞/LPV controller, the two following cases are considered:

- First case: **varying forward velocity** $\rho_1 \in [40\ \text{km/h}, 130\ \text{km/h}]$ and **fixed weighting functions** $\rho_{2,3} = 0.5$;
- Second case: **varying weighting functions** $\rho_{2,3} \in [0, 1]$ and **fixed forward velocity** $\rho_1 = 70$ km/h.

They are detailed in the sequel.

Table 1
Reduction of the magnitude of Transfer Functions (TF) compared with the passive case at 40 km/h and 130 km/h.

TF	$v = 40$ km/h	$v = 130$ km/h
$\frac{R_f}{\delta_f}$	11 dB [0, 4 rad/s]	18 dB [0, 5 rad/s]
$\frac{R_r}{\delta_f}$	14 dB [0, 10 rad/s]	16 dB [0, 10 rad/s]

5.1.1. First case: varying forward velocity $\rho_1 \in [40\ km/h, 130\ km/h]$ and $\rho_{2,3} = 0.5$

We only consider 10 grid points for the varying parameter $\rho_1 = v$. Fig. 3 shows respectively the transfer function magnitude of the normalized load transfers ($\frac{R_{f,r}}{\delta_f}$) and of the input currents $\frac{u_{f,r}}{\delta_f}$ at the two axles, as well as the inverse of the weighting functions ($\frac{1}{W_{zRf}}, \frac{1}{W_{zRr}}, \frac{1}{W_{zuf}}, \frac{1}{W_{zur}}$). As shown in Figs. 3*a, b* and Table 1, the LPV active anti-roll bar system allows to reduce the normalized load transfers (at the two axles) compared with the passive anti-roll bar system in the frequency range up to more than 4 rad/s, which represents the limited bandwidth of the driver [9].

Figs. 3*c, d* show the transfer function magnitude of the input currents at the front ($\frac{u_f}{\delta_f}$) and rear axles ($\frac{u_r}{\delta_f}$), respectively. When the forward velocity increases, the controller input currents ($u_{f,r}$) also increase, which means that more energy is required. Nonetheless, it remains in the allowed bound, which prevents the actuator saturation.

5.1.2. Second case: varying weighting functions $\rho_{2,3} \in [0, 1]$ and $\rho_1 = v = 70\ km/h$

We consider only 5 grid points for each of the varying parameters $\rho_{2,3}$. Fig. 4 shows the transfer function magnitude of the normalized load transfers at the two axles $\frac{R_{f,r}}{\delta_f}$ when the varying parameters $\rho_{2,3}$ are at the lower and upper bounds ($\rho_{2,3} = 0$ and $\rho_{2,3} = 1$).

As shown in Fig. 4, when the values of $\rho_{2,3}$ increase, the normalized load transfers at the two axles decrease in the frequency range up to more than 4 rad/s. The reduction is about 19 dB between $\rho_{2,3} = 0$ and $\rho_{2,3} = 1$.

The results above indicate that the proposed H_∞/LPV controller (with the parameter dependent weighting functions, including the nor-

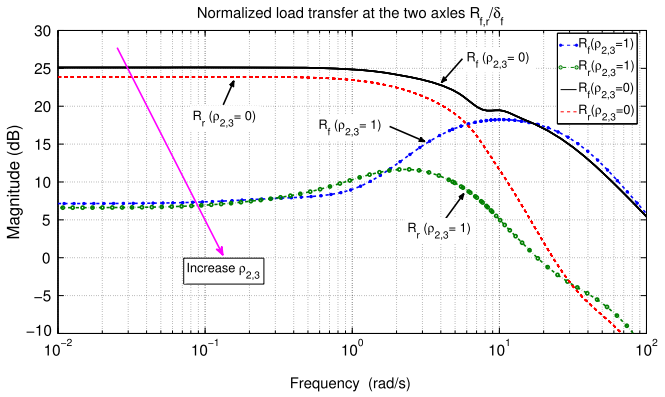

Fig. 4. Second case: transfer function magnitude of the normalized load transfers at the two axles $\frac{R_{f,r}}{\delta_f}$.

malized load transfers at the two axles) provides better performance adaptation to the rollover risk for heavy vehicles.

5.2. Time-domain analysis of the LPV control solution

In this section, the simulation results of the heavy vehicle using the four ESVH actuators with the parameter dependent weighting functions H_∞/LPV controller are shown in the time domain. The proposed controller is compared with two other controllers (H_∞/LTI, fixed weighting functions H_∞/LPV) and the passive anti-roll bar system.

5.2.1. Simulation scenario

To validate and to show the interest of the proposed H_∞/LPV controller strategy for the active anti-roll bar system with the 3 varying parameters $\rho_1 = v$, $\rho_2 = |R_f|$, $\rho_3 = |R_r|$, the following scenario is used:

- the vehicle manoeuvre is a double lane change, which is a typical case to evaluate an obstacle avoidance in an emergency. The manoeuvre has a 2.5 m path deviation over 100 m. The steering angle δ_f is shown in Fig. 5*a*.
- the vehicle runs on a dry road ($\mu = 1$). The total rolling and aerodynamic resistance forces are ignored.
- when the obstacle is detected, the driver reduces the throttle and brakes to reduce the forward velocity of the vehicle. The total braking force increases from 0.5 s to 1.5 s and then the driver takes off the brake pedal, as shown in Fig. 5*b*.

The differential equation for the forward velocity in the braking case is determined in equation (16) [7]:

$$m\dot{v} = -\sum_{i=1}^{4} F_{bi} \tag{16}$$

where F_{bi} is the braking force at the each wheel.

5.2.2. Roll stability analysis

Due to the braking force, the forward velocity reduces from $V_{Initial}$ = 90 km/h to $V_{Final} = 76.5$ km/h, as in Fig. 5*c*.

Figs. 5*c*, *d* show the variation of varying parameters $\rho = [\rho_1, \rho_2, \rho_3]$. Figs. 5*e*, *f* show the normalized load transfers at the two axles. In the case of the passive anti-roll bar system, rollover does occur indeed at the two axles, but not in the case of the H_∞/LPV controller: the maximum absolute values of the normalized load transfers at the front and rear axles are respectively 0.55 and 0.46. This shows that the H_∞/LPV controller improves significantly the roll stability of heavy vehicles compared with the passive anti-roll bar system. The force of the actuators, as well as the input current at the two axles, are shown in Fig. 5*g*, *h*.

Table 2
The value of $|R_r|_{max}$ for the rollover situation.

	$v_{Initial} \div v_{Final}$ (km/h)		
	65 ÷ 51	110 ÷ 96	130 ÷ 116
H_∞/LPV	0.22	0.5	**0.6**
H_∞/LPV (fixed WF)	0.3	0.75	**1 (Rollover)**
H_∞/LTI	0.4	**1 (Rollover)**	–
Passive	**1 (Rollover)**	–	–

5.2.3. Interest of the parameter dependent weighting functions H_∞/LPV controller on the roll stability

The forward velocity of the vehicle varies continuously during operation. Vehicle rollover often occurs when the forward velocity is within 60 to 110 km/h. In this section, one considers the forward velocity up to 130 km/h. Due to the braking force, when the initial velocity ($V_{Initial}$) varies from 40 to 130 km/h, the final velocity (V_{Final}) varies respectively from 26.7 to 116.7 km/h. The maximum absolute value of the normalised load transfers at the two axles $|R_{f,r}|_{max} < 1$ are used in order to assess the roll stability.

The proposed parameter dependent weighting functions H_∞/LPV controller (H_∞/LPV AARB) is compared with the following three cases:

- the fixed weighting functions H_∞/LPV controller (H_∞/LPV (fixed WF) AARB) with $\rho_{2,3} = 0.5$;
- the H_∞/LTI controller (H_∞/LTI AARB);
- the passive anti-roll bar system (Passive ARB).

Figs. 6, 7 show the effect of the forward velocity on the maximum absolute value of the normalised load transfers at the two axles $|R_{f,r}|_{max}$. We can see that the value of $|R_r|_{max}$ are higher than $|R_f|_{max}$, so the vehicle rollover occurs first at the rear axle.

Table 2 shows the value of the normalized load transfer at the rear axle $|R_r|_{max}$ for the rollover situation. In the case of the parameter dependent weighting functions H_∞/LPV controller, the maximum value of the normalized load transfers at the both axles are maintained under 0.6 when the forward velocity is $V_{Initial} = 130$, $V_{Final} = 116$ km/h.

By comparing with the H_∞/LTI and fixed weighting functions H_∞/LPV controller strategies, we can see that in the case of the parameter dependent weighting functions H_∞/LPV controller, the value of the normalized load transfers at the two axles are reduced. As the forward velocity increases, the efficiency of the dependent weighting functions H_∞/LPV controller becomes more pronounced.

The simulation results both in the frequency and time domains have shown the effectiveness of the parameter dependent weighting functions H_∞/LPV controller synthesis, which considered the three varying parameters: the forward velocity and the normalized load transfers at the two axles, compared with the three other cases.

6. Results & discussion

This section is devoted to the validation of the H_∞/LPV active anti-roll bar control by using the TruckSim®[1] simulation software.

TruckSim® delivers accurate, detailed, and efficient methods for simulating the performance of multi-axle commercial vehicles such as 4×2, 6×4 tractors as well as box trucks, buses and trailers. Let us note that it has been used in the literature in [18] to assess the effectiveness of the active roll control system of heavy vehicles.

To survey the proposed H_∞/LPV controller for the active anti-roll bar system with a nonlinear vehicle model, we use the co-simulation between Matlab®/ Simulink® and TruckSim® software, see Fig. 8. The nonlinear vehicle model is determined from the TruckSim® software,

[1] Mechanical Simulation Corporation, http://carsim.com/products/trucksim/.

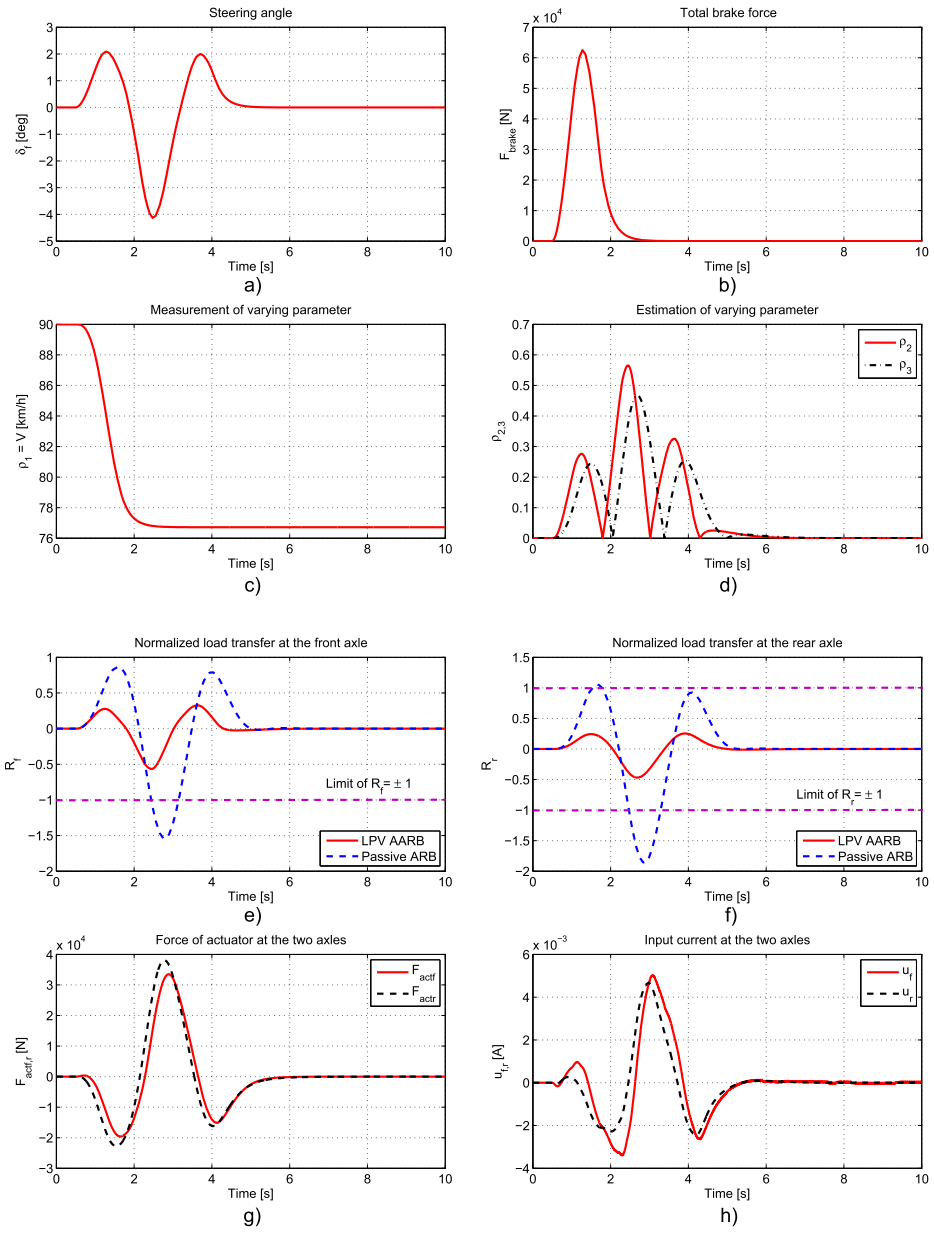

Fig. 5. Time responses of the heavy vehicle in the double lane change manoeuvre to avoid obstacle.

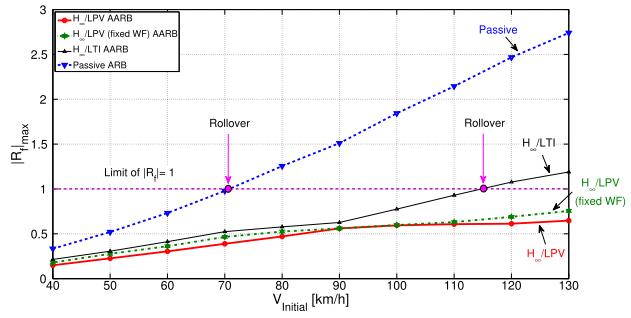

Fig. 6. Effect of the forward velocity on the maximum absolute value of the normalised load transfers at the front axle.

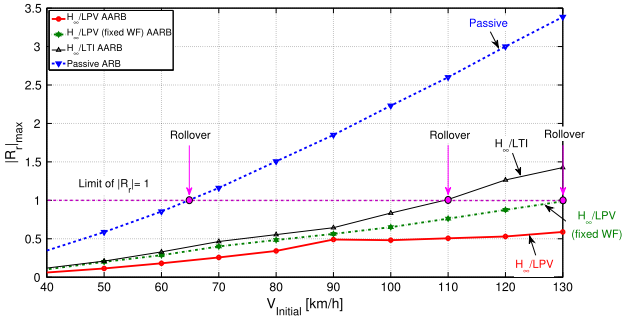

Fig. 7. Effect of the forward velocity on the maximum absolute value of the normalised load transfers at the rear axle.

integrated as a S-function in Simulink. Meanwhile, the controller and the actuators are built directly in the Matlab®/Simulink® environment.

In the sequel, the proposed H_∞/LPV controller is tested with two different types of vehicles: a fully loaded tour bus and a fully loaded LCF truck using the solid suspension system. The engine is mounted at the rear of the vehicle for the tour bus and at the front for the LCF truck. To evaluate the rollover of vehicles, we consider the tyre force (F_z) in the Z direction at the each wheel (rollover occurs when $F_z = 0$). Note that

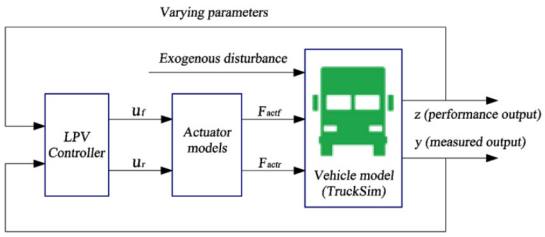

Fig. 8. Diagram of TruckSim®-Simulink® Co-Simulation.

the steering angle, in the following section, is the angle of the steering wheel, which is directly controlled by the driver. In the co-simulation between Matlab ®/Simulink® and TruckSim®, there are two possible solutions for the steering angle:

- first solution: the steering angle is made in Simulink® and entered to TruckSim® through the S-function. With this solution, the vehicle's trajectories in the cases of the passive and of the active anti-roll bar systems are often different, whether the wheels lift off the road or not.
- second solution: the steering angle is defined in TruckSim® with two scenarios:
  - the 1st one uses the closed-loop driver model, and the steering angle is automatically changed to adapt to the vehicle trajectory. Here, the vehicle's trajectories in the cases of passive and active anti-roll bar systems, will follow the target path which fits the driver's wishes. This scenario is used to define the steering angle for the tour bus;
  - the 2nd one uses the open loop driver model and the steering angles are the same for both the active and passive anti-roll bar systems. This scenario is used to define the steering angle for the LCF truck.

6.1. Validation with the tour bus

The commercial passenger buses are among the most popular people carrying vehicles in the world. Typically, they are two axled vehicles (bus 2A) with a capacity of 45 passengers, as shown in Fig. 9. In this validation, the total vehicle mass of the tour bus is 10620 kg and it runs at 100 km/h. The double lane change is used to evaluate the roll stability; this represents the situation when the driver wishes to overtake another vehicle. Figs. 10 and 11 show the time responses of the tour bus (continuous line for the H_∞/LPV active anti-roll bar system and dashed line for the passive anti-roll bar system).

Fig. 10 shows the steering wheel angle controlled by the driver with the amplitude about 100 deg. In ideal conditions, we would like that the centre of the vehicle mass follows the target path. However in reality, the trajectory of the centre of the vehicle mass of the real vehicle can not satisfy that (due to the impact of the suspension system, the wheelbase and the wheels lift off from the road, etc). Therefore the driver generates the steering wheel angle difference between the H_∞/LPV active anti-roll bar and the passive anti-roll bar systems. The trajectory of the vehicle, in the case of the H_∞/LPV active anti-roll bar system, is more sticked to the ideal target path compared with the passive anti-roll bar system as in Fig. 11*a*.

Figs. 11*b*, *c*, *d* show the time response of the roll angle of the sprung mass and the roll angle of the unsprung masses at the two axles, respectively. In the case of the H_∞/LPV controller, the roll angles of sprung and unsprung masses are significantly reduced when compared to the passive anti-roll bar system (about 6 deg for the sprung mass, 3 deg for the unsprung mass at the front and 4 deg for the unsprung mass at the rear axle).

Figs. 11*e*, *f*, *g*, *h* show the time response of the tyre forces in the Z direction of all the wheels. In the case of the H_∞/LPV controller, all the tyre forces remain positive, meaning that no wheel lifts off the road.

Fig. 9. Tour bus 2 axles (4 × 2).

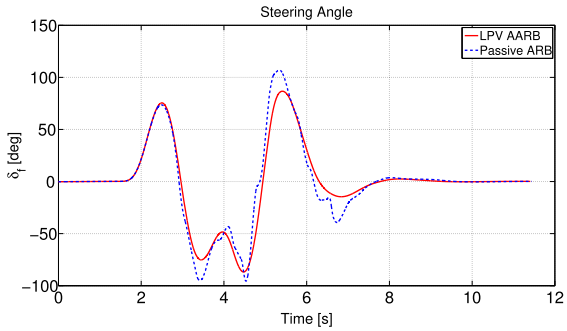

Fig. 10. Steering angle in the double lane change manoeuvre.

But in the case of the passive anti-roll bar, the left-front wheel lifts off at 2.6 s ÷ 3.4 s and 5.7 s ÷ 6.5 s, the right-front wheel at 3.8 s ÷ 5.3 s, the left-rear wheel at 5.8 s ÷ 6.5 s, the right-rear wheel at 4 s ÷ 5.5 s. These results show that the H_∞/LPV controller drastically improves the roll stability in the case of the fully loaded tour bus.

6.2. Validation with the LCF truck

In this validation, the total vehicle mass of the LCF truck (Fig. 12) is 12549 kg when it runs at 80 km/h. A sine wave steering manoeuvre is used to evaluate the roll stability. Figs. 13 and 14 show the time response of the vehicle (continuous line for the H_∞/LPV active anti-roll bar system and dashed line for the passive anti-roll bar system).

The driver applies the same steering wheel angles δ_f for both the H_∞/LPV active anti-roll bar and the passive anti-roll bar systems. It is a sine wave (amplitude of 90 deg and period of 4 s), as shown in Fig. 13. Fig. 14*a* shows the trajectory of the LCF truck. Even if the forward velocity is held constant at 80 km/h, the LCF truck travels to point A in the case of the passive anti-roll bar, and to point B in the case of the H_∞/LPV active anti-roll bar. Since the wheels lift off the road in the case of the passive anti-roll bar, some performance characteristics of the vehicle are lost.

Figs. 14*b*, *c*, *d* show that in the case of the H_∞/LPV controller, the roll angle of sprung and unsprung masses are significantly reduced compared to the case of the passive anti-roll bar (about 10 deg for the roll angle of sprung, 8 deg for the roll angle of the unsprung mass at the front axle, and 3 deg for the roll angle of the unsprung mass at the rear axle).

Figs. 14*e*, *f*, *g*, *h* show the time response of the tyre forces in the Z direction of all the wheels. In the case of the H_∞/LPV controller, all the tyre forces remain positive, meaning that no wheel lifts off the road. But in the case of the passive anti-roll bar, all the wheels at the two axles lift off. These results show that the H_∞/LPV controller improves the roll stability in the case of the fully loaded LCF truck.

The simulation results for both the tour bus and LCF truck show a drastic behavioural difference: the wheels at the front axle lift off the road before the wheels at the rear axle for the tour bus (see Fig. 11*g*, *h*). For the LCF truck, it is the opposite (see Fig. 14*g*, *h*). So the rollover risk is not the same for all types of heavy vehicles. Therefore, the proposed H_∞/LPV controller with the parameter dependent weighting functions

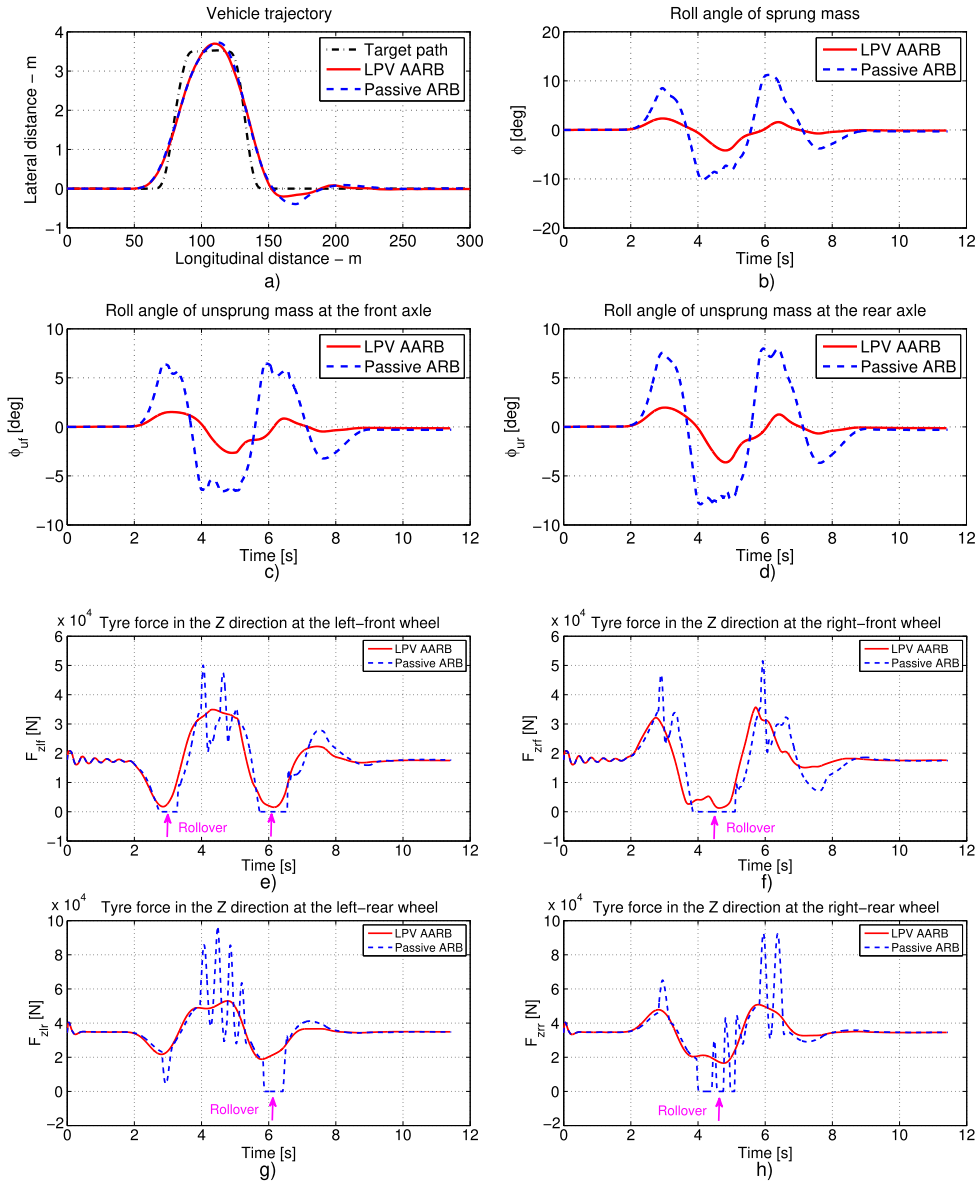

Fig. 11. Time responses of the tour bus in the double lane change manoeuvre.

Fig. 12. LCF truck 2 axles (4 × 2).

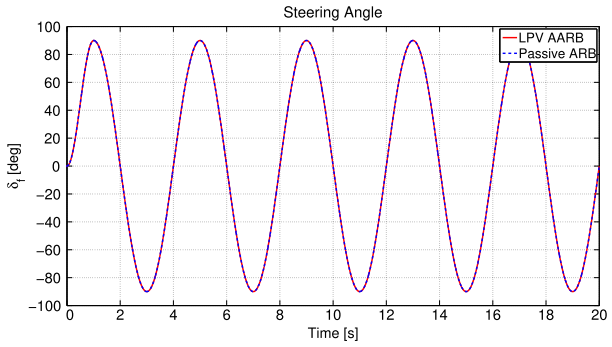

Fig. 13. Steering angle in the sine wave manoeuvre.

including the normalized load transfers at the two axles allows adapting the performance against the rollover risk for all types of heavy vehicles.

7. Conclusion

This paper proposed an LPV approach for the active anti-roll control of heavy vehicles. Together with an LPV vehicle model, some parameter dependent weighting functions are considered in the H_∞ context, leading to an LPV controller scheduled by three varying parameters: the forward velocity (v) and the normalized load transfers ($|R_f|$ and $|R_r|$) at the two axles.

The simulation results in the frequency and time domains as well as the validation by using the TruckSim® software show that the H_∞/LPV controller drastically improves the roll stability of the single unit heavy

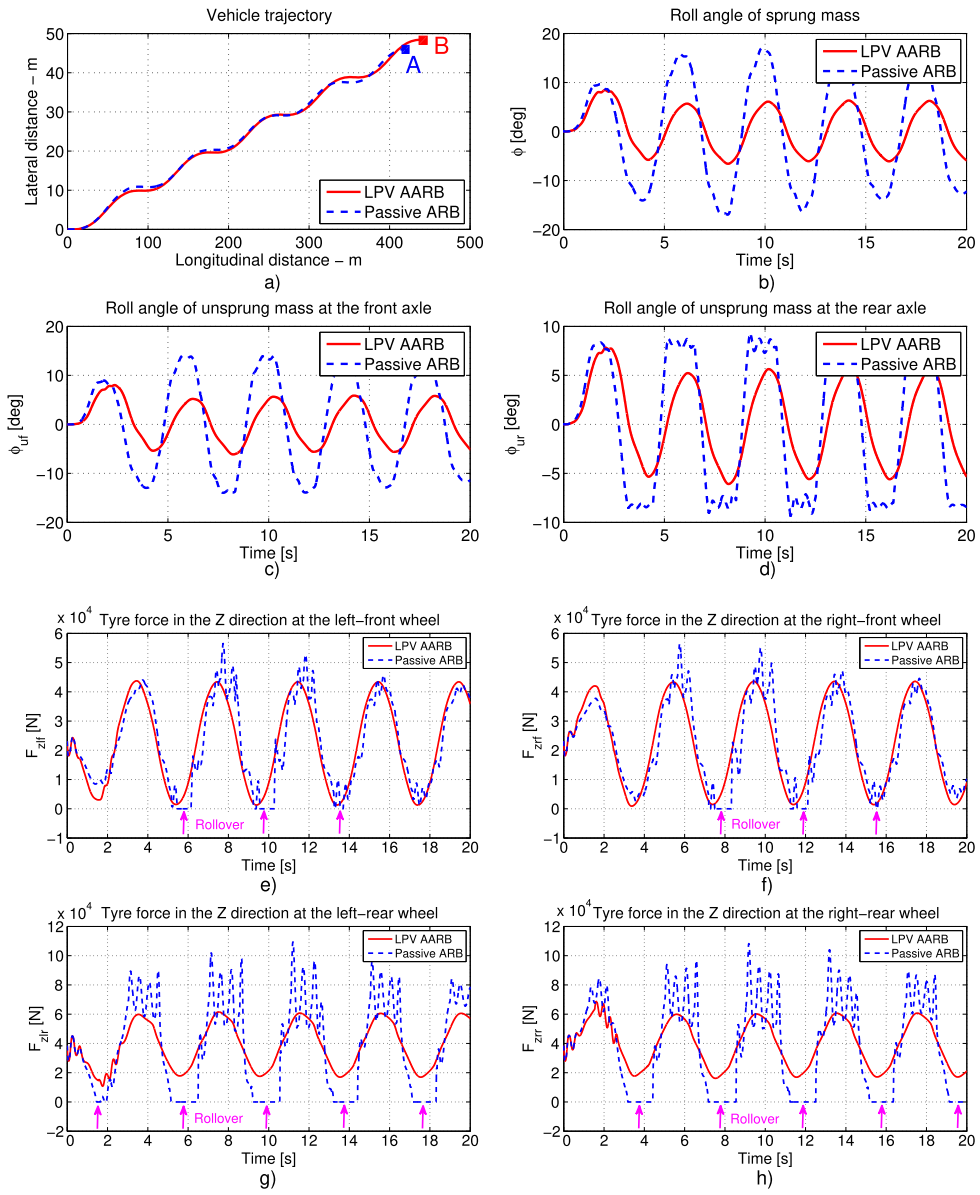

Fig. 14. Time responses of the truck in the sine wave steering manoeuvre.

vehicle when compared with the H_∞/LTI, the fixed weighting functions H_∞/LPV controllers and the passive anti-roll bar system.

So, the main interest of the H_∞/LPV design is to allow for performance adaptation to the risk of rollover of heavy vehicles. It is worth noting that this LPV strategy can be extended easily using other rollover indices as the ones proposed in [18].

Future works may concern the effect of the oil passing through the electronic servo-valve on the closed-loop system by using a LPV approach for fault tolerant control design.

Declarations

Author contribution statement

Van Tan Vu: Conceived and designed the experiments; Wrote the paper.

Olivier Sename, Luc Dugard: Analyzed and interpreted the data; Contributed reagents, materials, analysis tools or data.

Peter Gaspar: Performed the experiments.

Funding statement

This work was supported by the University of Transport and Communications through the key project (T2019-CK-012TD).

Competing interest statement

The authors declare no conflict of interest.

Additional information

No additional information is available for this paper.

References

[1] A. Miege, D. Cebon, Design and implementation of an active roll control system for heavy vehicles, in: 6th International Symposium on Advanced Vehicle Control, AVEC 2002, Hiroshima, Japan,, 2002.

[2] H. Imine, L.M. Fridman, T. Madani, Steering control for rollover avoidance of heavy vehicles, IEEE Trans. Veh. Technol. 61 (8) (2012) 3499–3509.

[3] D. Odenthal, T. Bunte, J. Ackermann, Nonlinear steering and braking control for vehicle rollover avoidance, in: European Control Conference, Germany, 1999.

[4] D.J. Cole, Fundamental issues in suspension design for heavy road vehicles, Vehicle System Dynamics, Int. J. Veh. Mech. Mobil. 35 (4–5) (2001) 319–360.
[5] M. Ieluzzi, P. Turco, M. Montiglio, Development of a heavy truck semi-active suspension control, Control Eng. Pract. 14 (3) (2006) 305–312.
[6] D.J.M. Sampson, Active Roll Control of Articulated Heavy Vehicles, Ph.D. thesis, University of Cambridge, UK, 2000.
[7] P. Gaspar, J. Bokor, I. Szaszi, The design of a combined control structure to prevent the rollover of heavy vehicles, Eur. J. Control 10 (2) (2004) 148–162.
[8] D. Sampson, D. Cebon, Active roll control of single unit heavy road vehicles, Veh. Syst. Dyn., Int. J. Veh. Mech. Mobil. 40 (4) (2003) 229–270.
[9] D. Sampson, D. Cebon, Achievable roll stability of heavy road vehicles, Proc. Inst. Mech. Eng., Part D, J. Automob. Eng. 217 (2003) 269–287.
[10] S. Fergani, O. Sename, L. Dugard, An LPV/H_∞ integrated vehicle dynamic controller, IEEE Trans. Veh. Technol. 65 (4) (2016) 1880–1889.
[11] J. Mohammadpour, C. Scherer, Control of Linear Parameter Varying Systems with Applications, Springer, 2012.
[12] O. Sename, P. Gaspar, J. Bokor, Robust Control and Linear Parameter Varying Approaches: Application to Vehicle Dynamics, Springer, 2013.
[13] V. Vu, O. Sename, L. Dugard, P. Gaspar, Enhancing roll stability of heavy vehicle by lqr active anti-roll bar control using electronic servo-valve hydraulic actuators, Vehicle System Dynamics, Int. J. Veh. Mech. Mobil. 55 (9) (2017) 1405–1429.
[14] D. Sampson, D. Cebon, An investigation of roll control system design for articulated heavy vehicles, in: 4th International Symposium on Advanced Vehicle Control, AVEC1998, Nagoya, Japan, 1998.
[15] A. Miege, D. Cebon, Optimal roll control of an articulated vehicle: theory and model validation, Vehicle System Dynamics, Int. J. Veh. Mech. Mobil. 43 (12) (2005) 867–884.
[16] V. Vu, O. Sename, L. Dugard, P. Gaspar, Active anti-roll bar control using electronic servo-valve hydraulic damper on single unit heavy vehicle, in: IFAC Symposium on Advances in Automotive Control – 8th AAC 2016, Norrköping, Sweden, 2016.
[17] P. Gaspar, J. Bokor, I. Szaszi, Reconfigurable control structure to prevent the rollover of heavy vehicles, Control Eng. Pract. 13 (6) (2005) 699–711.
[18] H. Yu, L. Guvenc, U. Ozguner, Heavy duty vehicle rollover detection and active roll control, Vehicle System Dynamics, Int. J. Veh. Mech. Mobil. 46 (6) (2008) 451–470.
[19] H. Hsun-Hsuan, K. Rama, A.G. Dennis, Active roll control for rollover prevention of heavy articulated vehicles with multiple-rollover-index minimisation, Vehicle System Dynamics, Int. J. Veh. Mech. Mobil. 50 (3) (2012) 471–493.
[20] F. Wu, Control of Linear Parameter Varying Systems, Ph.D. thesis, University of California at Berkeley, USA, 1995.
[21] F. Wu, A generalized LPV system analysis and control synthesis framework, Int. J. Control 74 (7) (2001) 745–759.
[22] F. Wu, X.H. Yang, A. Packard, G. Becker, Induced L2-norm control for LPV systems with bounded parameter variation rates, Int. J. Robust Nonlinear Control 6 (9–10) (1996) 983–998.
[23] C. Hoffmann, H. Werner, Complexity of implementation and synthesis in linear parameter-varying control, in: IFAC World Congress – 19th IFAC WC 2014, Cape Town, South Africa, 2014.
[24] A. Packard, Gain scheduling via linear fractional transformations, Syst. Control Lett. 22 (2) (1994) 79–92.
[25] P. Apkarian, P. Gahinet, A convex characterization of gain-scheduled H_∞ controllers, IEEE Trans. Autom. Control 40 (5) (1995) 853–864.
[26] G. Becker, Quadratic Stability and Performance of Linear Parameter Dependent Systems, Ph.D. thesis, University of California at Berkeley, USA, 1993.
[27] A. Hjartarson, P. Seiler, A. Packard, LPVtools: a toolbox for modeling, analysis, and synthesis of parameter varying control systems, in: First IFAC Workshop on Linear Parameter Varying Systems, France, 2015.
[28] A. Marcos, G.J. Balas, Development of linear-parameter-varying models for aircraft, J. Guid. Control Dyn. 27 (2) (2004) 218–228.
[29] S. Hecker, Generating structured LPV-models with maximized validity region, in: IFAC World Congress – 19th IFAC WC 2014, Cape Town, South Africa, 2014.